C. Primaz, O. Gil-Castell, A. Ribes-Greus. Partial glycolytic depolymerisation of poly(ethylene terephthalate) (PET) in the solid state: modelling the contribution of time and temperature. Polymer Degradation and Stability 2024:221;110695

Partial glycolytic depolymerisation of poly(ethylene terephthalate) (PET) in the solid state: modelling the contribution of time and temperature

S. F. Llopis[1,*], E. Verdejo[1], O. Gil-Castell[2,*], A. Ribes-Greus[2]

[1]AIMPLAS, Gustave Eiffel 4, 46980 Paterna, Spain

[2]Instituto de Tecnología de Materiales (ITM), Universitat Politècnica de València (UPV), Camino de Vera s/n, 46022 Valencia, Spain

[*]Corresponding author:

O. Gil-Castell ogilcastell@doctor.upv.es, A. Ribes-Greus aribes@ter.upv.es

Partial glycolytic depolymerisation of poly(ethylene terephthalate) (PET) in the solid state: modelling the contribution of time and temperature

S. F. Llopis[1,*], E. Verdejo[1], O. Gil-Castell[2,*], A. Ribes-Greus[2]

[1]AIMPLAS, Gustave Eiffel 4, 46980 Paterna, Spain

[2]Instituto de Tecnología de Materiales (ITM), Universitat Politècnica de València (UPV), Camino de Vera s/n, 46022 Valencia, Spain

[*]Corresponding author: s.llopis@aimplas.es; oscar.gil@uv.es

Abstract

Glycolysis is one of the most explored approaches to the chemical recycling of poly(ethylene terephthalate) (PET). Apart from complete depolymerisation, which is the traditional strategy in this field, there is also the possibility of partial depolymerisation of PET in the solid state so that instead of reaching the monomer, oligomeric and polymer chains with a tuneable polymerisation degree are formed. This study monitored and modelled the partial depolymerisation of PET using an excess of ethylene glycol (EG) in the absence of an additionally added catalyst (only remnant production catalysts) at different times (from 10 to 120 min) and temperatures (from 160 to 210 °C) as a feasible approach for tailoring physico-chemical performance of PET fractions. Under these conditions, glycolysis involved the heterogeneous process concerning the diffusion of EG into the bulk PET particles and attack of amorphous regions, coexisting with the beginning of the homogeneous stage with the further generation of oligomers and a minor number of BHET molecules. Monitoring glycolysis highlighted variations in the solid fraction of PET: a significant molar mass reduction, an increase in polar hydroxyl groups, and promotion of low-lamellar thickness crystalline population. These changes were empirically modelled using a Boltzmann equation and offering the possibility of tailoring the physico-chemical performance of PET as a function of immersion time and temperature for this particular system. The glycolysed fractions of PET waste can be considered appropriate for closed-loop, semi-closed, and open-loop chemical recycling, with different applications through a simple, green, and versatile process.

Keywords

Glycolysis, poly(ethylene terephthalate), chemical recycling, tailoring properties

1. Introduction

The global production of plastics reached 391 million tonnes in 2021, being the packaging sector one of the largest end-use markets (44%). In Europe, more than 57 million tonnes of plastics were produced, of which more than 50% were managed as post-consumer waste. Although great effort is being made for plastic post-consumer waste collection, 23% still ended up in landfills, 42% were incinerated and 35% were mechanically recycled [1]. Even if plastic waste collection improved meaningfully, mechanical recycling limitations provoked that a significant percentage still ends up in landfills or is destined for energy recovery. Therefore, developing technological alternatives complementary to mechanical recycling is crucial to increasing the circularity of plastic waste.

Among plastics applied to the packaging sector, poly(ethylene terephthalate) (PET) is regarded as the fourth most used, below poly(ethylene) (PE), poly(propylene) (PP) and poly(vinyl chloride) (PVC) [1]. Including fibres for textiles, PET becomes the second in the most used polymers ranking. PET is the most relevant member of the linear aromatic polyesters family and has become a primary daily-used material due to its appropriate properties such as durability, versatility and lightness [2]. One of the widely extended uses of PET is for manufacturing products with a single use that are discarded in a short period. Such a scenario provokes economic, environmental and social concerns that encourage managing PET wastes according to circular economy principles [3,4]. Current advances in the valorisation of PET encompass a spectrum of approaches. Enzymatic depolymerisation methods are progressing with improved enzymes and optimized conditions [5,6], microwave-assisted depolymerization is becoming more energy-efficient and selective [7,8], and mechanical recycling is evolving with advanced grinding techniques, additive integration, high-throughput processes, and integrated chemical modifications [9,10]. These advancements collectively contribute to more sustainable and effective PET recycling strategies across various technological fronts. Despite these advances, especially in mechanical recycling, there is still a significant proportion that still ends up in landfills or is destined for energy recovery, due to technology readiness limitations or process drawbacks. Therefore, developing technological alternatives is necessary to comply with circular economy principles, the 2030 Agenda [5], and the Sustainable Development Goals (SDGs) from the United Nations [6].

Among others, there is an increasing trend for depolymerising PET residues and reintroducing them into the production stream of speciality products such as saturated and unsaturated polyester resins, coating materials, additives and polyurethanes or fuels [11,12]. Chemical

recycling ultimately involves breaking the polymer chain through depolymerisation, producing raw monomers for new polymer production and other value-added by-products [13–15]. Some of the most relevant chemical recycling strategies for PET involve glycolysis, hydrolysis, methanolysis, aminolysis or hydrogenation, depending on the chemical agent used to cleave the polymer chain [16]. Among them, glycolysis by ethylene glycol (EG) is one of the most common methods for the chemical recycling of PET because it allows the use of minimal amounts of reagents and milder conditions (pressures and temperatures) compared to other techniques [17–20]. This mildness contributes to the overall sustainability of the process by minimizing energy consumption and the generation of harmful by-products. Moreover, ethylene glycol is a relatively inexpensive and commercially available chemical that can be produced from renewable feedstocks, such as biomass or bio-based sources, aligning with the principles of green chemistry and reducing dependence on fossil fuels [21,22]. This, together with the cost is particularly crucial for large-scale industrial applications where cost considerations play a significant role. Ethylene glycol also exhibits versatility as it is compatible with existing industrial infrastructure and can be recovered and reused in the process, thus involving low waste generation [23].

Glycolysis is one of the most attractive systems for the chemical recycling of PET into bis-2-hydroxyethyl terephthalate (BHET), which can be subsequently used for the preparation of new PET. Without a catalyst, this process results from multiple alcoholysis and transesterification reactions that occur in a single homogeneous phase involving long times at temperatures higher than 245 °C [24–26]. At lower temperatures, glycolysis of PET occurs in the solid state during dispersion in a liquid phase [27,28]. Compared to some alternative methods for PET valorisation, the glycolytic process using ethylene glycol tends to have a lower environmental impact. It produces fewer harmful by-products and can contribute to a closed-loop recycling system where PET can be recycled into new products.

The overall PET glycolysis process may be summarised in the following stages, as schematised in **Fig. 1**: (*i*) diffusion of EG into the bulk of PET particles; (*ii*) attack to amorphous regions and generation of oligomers; (*iii*) further generation of oligomers and a small number of BHET molecules in the amorphous regions still involving separated solid and liquid phases; (*iv*) fragmentation into prominently crystalline small entities of oligomers; (*v*) solubilisation of oligomers into the liquid phase; and (*vi*) generation of BHET molecules.

In addition to the complete depolymerisation of the polymer into its respective monomers, there is also the possibility of partial depolymerisation of solid PET in bulk when applying milder glycolysis conditions so that intermediate-molar mass chains are formed. Although BHET yield is scarce in the early stages of the glycolysis reaction, the solid fraction of PET is subjected to several reactions that promote changes in its structure and morphology [29]. Particularly for the glycolytic treatment of PET, the heterogeneous process that lately coexists with the homogeneous phase previously described in stages (*i*) to (*iii*) can be considered a promising opportunity for tailoring the physico-chemical properties of PET waste [18]. In this regard, empirically modelling the changes in the performance as a function of glycolysis time and temperature would be very useful for preparing glycolysed fractions of a particular behaviour on demand.

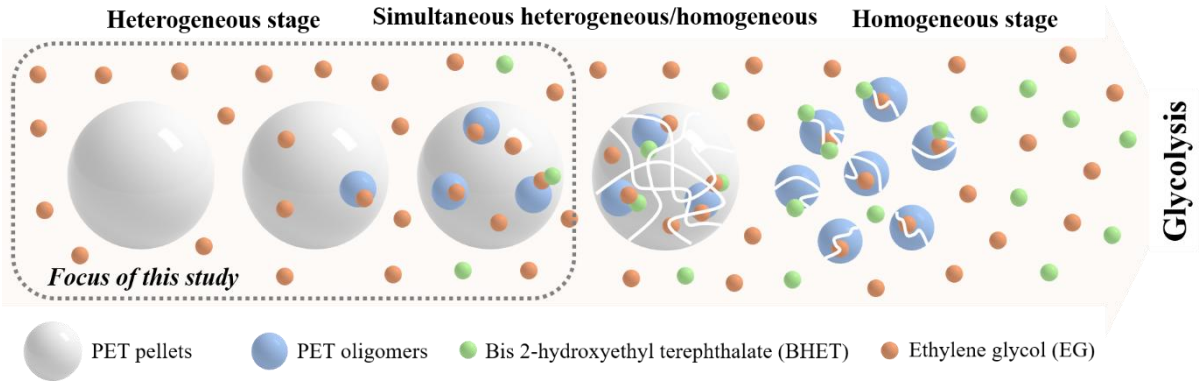

Fig. 1. Macroscopic scheme for the glycolysis of PET, with indications of the focus of this study.

According to their physico-chemical behaviour, glycolysed polymer chains can be considered appropriate for closed-loop recycling, semi-closed loop and open-loop recycling, with different applications of varying value. On the one hand, partial depolymerization allows for the recycling of solid PET while preserving a significant portion of its original polymer properties. This is crucial for closed-loop strategies, where the goal is to maintain the quality of the material and reuse it in similar high-value applications. Moreover, compared to full depolymerization, partial depolymerization may require less energy input, which is essential for sustainability and cost-effectiveness. In semi-closed loop systems specific polymers are selectively targeted and recovered from mixed plastic waste streams. This targeted recovery is essential for ensuring the quality and purity of recycled materials, especially when dealing with complex mixtures. Semi-closed loop systems allow for the maintenance of material quality by selectively recovering and recycling specific polymers without subjecting them to excessive processing. This is particularly important for applications where high-quality recycled materials are required.

Moreover, semi-closed loop systems can be frequently adapted to existing recycling facilities and infrastructure. This adaptability minimizes the need for extensive modifications or the construction of entirely new facilities, making it a more feasible option for transitioning from open-loop to closed-loop practices. Finally, open-loop recycling involves processing plastic waste into new materials with potentially different applications. Partial depolymerization provides a versatile intermediate stage, producing valuable tailored-size polymer molecules that can be further processed into a range of products, enhancing the adaptability of the open-loop recycling system. Partial depolymerization can also simplify downstream processing steps in open-loop systems by producing intermediates with lower molecular weights. This can reduce the complexity of purification and polymerization processes in the production of new materials.

Examples of these strategies can be found in the literature, where the glycolysed PET fractions of higher molar mass can be used as raw materials for downgraded applications, as components in blends, and as matrix and/or reinforcing agents in thermoplastic or thermosetting materials [30–34]. Oligomers with lower molar mass can be considered for polycondensation of PET pre-polymers [35–37], modified with chain extenders for the preparation of thermosetting copolymers [38,39], or as additives for favouring enzymatic degradation of PET [40], among others.

Therefore, this study aims to monitor and model the partial glycolytic depolymerisation of PET in the solid state using an excess of EG in the absence of an additionally added catalyst (only remnant production catalysts) at different times (from 10 to 120 min at 180 °C) and temperatures (from 160 to 210 °C during 30 min) as a feasible approach for accurate tailoring the physico-chemical properties of PET wastes. Hence, the comprehensive study of the changes in the solid fraction in the early stages of glycolysis during the heterogeneous phase involves the novelty of this work, which is presented as a promising opportunity for preparing PET fractions with a specific performance by applying a simple glycolytic strategy.

2. Materials and methods

2.1. Materials, reagents and glycolysis strategy of PET

Commercial PET pellets (d < 2 mm) with M_w 25000 g·mol^{-1} and intrinsic viscosity 0.58 dL·g^{-1} were supplied by Novapet (Zaragoza, Spain). Ethylene glycol ReagentPlus® ≥99%, 1,1,1,3,3,3-Hexafluoro-2-propanol ≥99% (HFIP) and sodium trifluoroacetate 98% were purchased from Sigma Aldrich (St. Gallen, Switzerland) and used without further purification. PET pellets were dried under vacuum at 50 °C overnight.

Glycolysis of PET was carried out in a 500 cm^3 three-necked flat-bottom glass reactor equipped with a thermometer and a reflux condenser operated at atmospheric pressure. The reaction vessel and the EG solution were preheated to the selected temperature before adding the PET granules to minimise the time required to reach the reaction temperature. In all runs, 10 g of dry PET pellets involving an EG:PET molar ratio of 4:1 were introduced into the reactor. On the one hand, the glycolysis reaction proceeded for 10, 20, 30, 60, 90 and 120 min at 180 °C. On the other hand, the reaction was carried out at 160, 170, 180, 190, 200 and 210 °C for 30 min. After the specific time interval at the reaction temperature, the reactor vessel was removed from the heating mantle, quenched quickly in an ice bath, and the suspension was filtered. The product was separated into solid and liquid phases using Whatman glass microfiber binder-free filters, grade GF/C-1.2 mm (Maidstone, UK), under vacuum. The glycolysed samples were obtained as a solid phase retained after subsequent stages of filtration and washing with ultrapure water, altogether resulting in a solid yield above 97%. This solid yield was calculated with **Eq. 1**, where m_0 is the initial mass and m_d is the mass obtained after a drying stage of the filtrate in an oven at 60 °C for 12 h. The products obtained were then micronized in a dry mill microniser using Retsch ZM 200 Ultra Centrifugal Mill (Haan, Germany) under an N_2 atmosphere.

$$Yield\ (\%) = \frac{m_0 - m_d}{m_0} \cdot 100 \qquad (1)$$

2.2. Scanning electron microscopy (SEM)

The consequences after the glycolytic treatment were visually analysed by field-emission scanning electron microscopy (FE-SEM) in a Hitachi S4800 equipment. For this purpose, the dry-treated entire PET pellets and the cross-section portions obtained after transverse cutting with a scalpel were deposited onto sample holders and sputter-coated with a platinum layer for 60 s. Finally, the surface micrographs were taken using a voltage of 3 kV.

2.3. Fourier-Transform infrared spectroscopy (FT-IR)

The chemical structure was studied using Fourier-Transform infrared spectroscopy (FT-IR) analysis in the attenuated total reflectance (ATR) mode. In detail, a ThermoFischer iS50 spectrometer (Waltham, MA, USA) was considered, and spectra were collected in the wavenumber range between 500 to 4000 cm^{-1}, with a resolution of 4 cm^{-1} during 64 accumulations. Five analyses per sample were performed and averaged with the aid of the Omnic® software. For normalisation purposes, the proportion of the absorbance of the C–O

and O–H stretching signals at 1240 and 3425 cm^{-1} versus the peak at 1410 cm^{-1} of the in-plane deformation of the benzene ring was considered, which is usually regarded as an internal standard in PET infrared spectroscopy studies [41,42]

2.4. Gel permeation chromatography (GPC)

A Waters 1515 liquid chromatograph (Milford, MA, USA) equipped with a Waters 717 plus autosampler, a photodiode array detector (PDA 2998) and a Phenomenex Phenogel 5 μm linear column (300×7.8 mm) (Torrance, CA, USA) was used to measure the molar mass distribution at room temperature. HFIP with 10 mM sodium trifluoroacetate was used as the eluent at a flow rate of 1 $mL \cdot min^{-1}$ and as the solvent. Poly(methyl methacrylate) (PMMA) standards with 10 narrowly distributed molar masses were used to calibrate the system. All the polymer solutions were prepared in triplicates with a concentration of 0.2 wt.% and were filtered through a 0.22 μm PTFE syringe filter before injection. The molar mass distributions were analysed using the Empower 4 software.

2.5. Thermogravimetric analysis (TGA)

The thermo-oxidative stability was assessed through thermogravimetric analysis (TGA) in a Mettler-Toledo TGA 851 series setup (Columbus, OH, USA). The samples, with a mass of about 4 mg, were introduced into 70 μL Mettler-Toledo perforated alumina crucibles. A dynamic heating program with a rate of 10 $°C \cdot min^{-1}$ from 25 to 800 °C was applied in an oxygen atmosphere, with a flux of 50 $mL \cdot min^{-1}$. The samples were analysed in triplicates, and averages and deviations were taken as representatives.

2.6. Differential scanning calorimetry (DSC)

The thermal properties were analysed using differential scanning calorimetry (DSC) in a Mettler-Toledo DSC 820e device (Columbus, OH, USA). The samples with a 4 mg mass were deposited in perforated aluminium crucibles of 40 μL. Analyses were carried out from 0 °C to 280 °C with a heating rate of 10 $°C \cdot min^{-1}$ under an inert atmosphere of N_2, with a flux of 50 $mL \cdot min^{-1}$. The samples were analysed in triplicates, and averages and deviations were taken as representatives.

The crystallinity degree (X_c) was calculated through **Eq. 2**.

$$X_c(\%) = \frac{\Delta h_m - \Delta h_{cc}}{\Delta h_m^0} \times 100 \qquad (2)$$

where Δh_m and Δh_{cc} are the measured melting enthalpy and cold crystallisation enthalpy, and Δh_m^0 is the heat of fusion of 100% crystalline PET (140 J·g^{-1}) [43].

The lamellar thicknesses (l_c) were calculated by applying the Thomson-Gibbs equation (**Eq. 3**) based on the temperatures associated with the melting transitions [44–46],

$$l_C(T_m) = \left[\left(1 - \frac{T_m}{T_m^0}\right) \cdot \frac{\Delta h_{mV}}{2 \cdot \sigma_e}\right]^{-1} \quad (3)$$

where T_m is the melting peak temperature; T_m^0 is the equilibrium melting temperature of an infinite crystal (564 K); σ_e is the surface free energy of the basal plane where the chains fold (0.106 J·m^{-2}); and Δh_{mV} is the melting enthalpy per volume unit (2.1·10^8 J·m^{-3}) [47].

3. Results and discussion

3.1. Morphological modifications during glycolysis

The degradation of polymers as a consequence of the interaction with another chemical specie typically involves the process of chain cleavage. According to the penetration rate of the agent, the degradation rate of the polymer's functional groups and the matrix dimensions, the degradation process may induce changes in the surface morphology, and also in the inner part of the particles involving both surface and bulk degradation processes [48]. While surface degradation involves chemical reactions occurring at the outer layers, leading to modifications in surface morphology and chemistry, bulk degradation involves the cleavage of bonds throughout the polymer matrix, preferentially in the amorphous regions, resulting in the formation of smaller oligomeric fragments [49]. Therefore, the study of the surface and interior appearance as a function of glycolysis conditions may allow for a visual identification of the consequences of the process. **Fig. 2** shows the surface and cross-section electron micrographs of the raw PET and treated pellets at 180 °C during 30, 60 and 120 min, and at 210 °C during 30 min. These samples were particularly selected to highlight the effects of time and temperature, respectively, on the surface of the PET pellets.

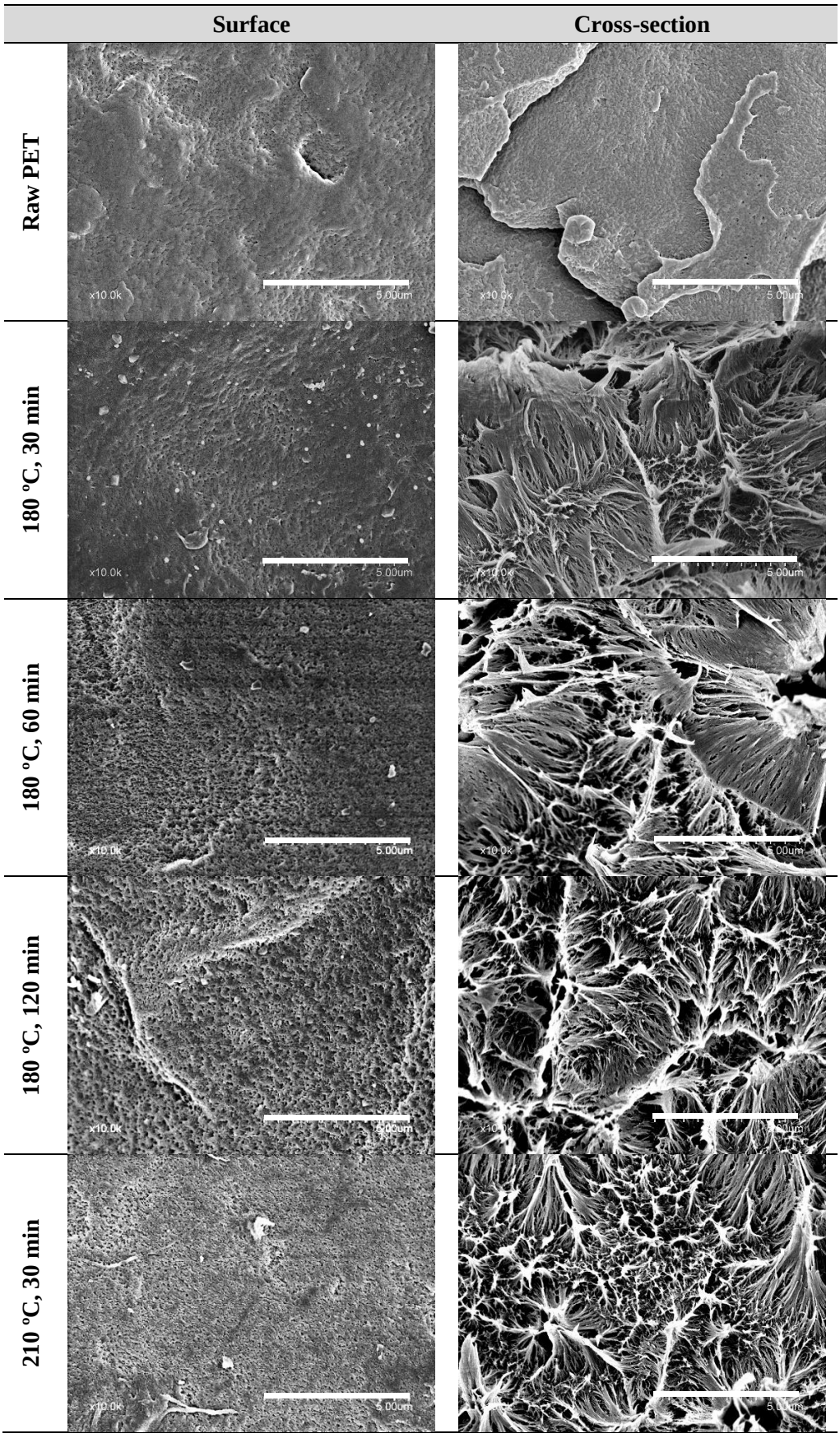

Fig. 2. Surface (left) and cross-section (right) morphology of the PET pellets for selected times and temperatures. Magnification set at 10000×; scale bar is equivalent to 5 μm.

It can be observed that glycolysis treatment resulted in the roughening and etching of the surface and the formation of irregular structures. The surface microstructure of PET pellets also experienced alterations during exposure to ethylene glycol, including the formation of pits and nanovoids. These changes, recognised as a consequence of the chemical reactions and cleavage of polymer chains occurring at the surface, related to surface degradation processes, were more accentuated as a function of temperature and especially promoted as a function of time.

As for the interior of the pellets, a drastic change in the morphology was identified. Whereas the raw PET showed a compact structure with some minor voids, all the pellets subjected to glycolysis treatment revealed a distinctive morphology with a ramified-like appearance. This structure is compatible with the spherulitic crystalline structure of PET and may be a result of the elimination of the interlamellar amorphous regions. The amorphous and crystalline regions of PET can have different susceptibilities to degradation [50]. Generally, amorphous regions are often targeted preferentially due to their higher accessibility and reactivity, which provide more sites for degradation because of their less ordered and more open structure, making them more susceptible to chemical reactions [51,52]. Crystalline regions, on the other hand, may have a more ordered structure, more difficult to penetrate and are consequently less reactive [53,54]. However, it's important to note that the overall degradation process can involve both amorphous and crystalline regions to varying extents [49]. The specific conditions of the glycolysis reaction, such as temperature or time, can also influence the extent to which amorphous or crystalline regions are degraded.

Therefore, it was demonstrated that the glycolysis of PET carried out in this work involved both bulk and surface degradation processes, preferentially in the amorphous domains, the prevalence of which has a close relation to the glycolysis conditions. Particularly, temperature has been shown to have a critical role in this matter, as it can modulate the sorption and diffusion rates of the ethylene glycol to the PET particles. In particular, for fast penetration rates of ethylene glycol, the material rapidly swells and incorporates the chemical agent into the whole structure, thus resulting in a prevalent bulk degradation process, always in combination with surface degradation in the external region of the particles. In this regard, adjusting the reaction temperature can influence the kinetics of glycolysis and promote the prevalence of either bulk or surface degradation processes. As expected, greater times for a given temperature also accentuated the consequences of the glycolytic treatment in bulk. Deeper insights on the degradation performance of PET are given in the next sections.

3.2. Structural changes in the solid fraction induced by glycolysis

The glycolysis of PET in the solid fraction was next monitored from a spectroscopic perspective to evaluate the variation of the signals ascribed to functional groups as a result of chain scission and transesterification reactions. The complete FT-IR spectra in the wavenumber range of 4000 to 400 cm^{-1} as a function of glycolysis time and temperature are shown in **Fig. 3a**, while **Fig. 3b** and **3c** show in detail the regions from 1500 to 900 cm^{-1} and from 3800 to 3200 cm^{-1}.

From the global spectra, a new broad band was appreciated at 3300-2500 cm^{-1} due to O−H stretching and the promotion of −OH terminated species when glycolysis progressed. Moreover, greater intensity of the band at 1715 cm^{-1} of the C=O stretching from the carbonyl groups and more peak prominence at 1340 cm^{-1} caused by O−H bending could be appreciated. These signs, representing the generation of glycolysed shorter segments, oligomers and BHET, are characteristic of the glycolytic degradation of PET [55].

The detailed spectra in the region of from 1500 to 900 cm^{-1} and from 3800 to 3200 cm^{-1} corroborate that higher immersion time and elevated temperatures enhanced the glycolytic breakage of PET macromolecules. Notably, it was perceived greater absorbance of the bands at 1240 cm^{-1} and 1090 cm^{-1} due to the stretching of C−O from aromatic esters and primary alcohols, respectively. Moreover, the strong band around 3280 cm^{-1} has been ascribed specifically to BHET [56]. Finally, the bands in the region from 3600 to 3300 cm^{-1} demonstrated the O−H stretching of free and intermolecular bonded units.

Therefore, as a result of the heterogeneous solid-state process undergone in the particles of PET during immersion [18,26,57], the assessed insoluble solid fraction at the end of glycolysis treatment contained a combination of degradation by-products involving BHET, dimers, oligomers and PET macromolecules, which have been reported to exist in equilibrium [11,58–61]. Although most of the BHET, dimers and trimers with typically hydroxyl end groups may be eliminated during filtering and washing of the remnant solid fraction after glycolysis, it is suggested that at the glycolysis extent of this study, they remained retained inside the solid particles as schematised in **Fig. 1**, and according to morphological changes shown in the previous section. In this scenario, the trapping of oligomeric species into the PET pellets during glycolysis primarily occurs due to the physical and chemical interactions taking place within the polymer matrix. From a physical perspective, the formed oligomeric species during glycolysis, being smaller fragments, can become entrapped within the spaces and voids of the PET matrix. This, together with the limited mobility of oligomeric species especially within the

solid crystalline PET structure, contributes to the above-mentioned trapping of oligomers within the PET solid particles. From a chemical point of view, the glycolysis process of PET leads to the formation of reactive intermediates. These intermediates can include hydroxyl and carboxyl groups on the polymer chains and oligomeric fragments, which may chemically react with the functional groups present on the PET polymer chains or other oligomers. This chemical bonding anchors the oligomeric fragments to the PET matrix, preventing their easy release. Moreover, in some cases, the glycolytic process may result in the formation of cross-links within the PET structure. These cross-links can physically trap oligomeric species by connecting different segments of the polymer matrix.

Deeper insights into the effects of glycolysis conditions were achieved when assessing the normalised absorbance of the C−O and O−H stretching signals at 1240 and 3425 cm^{-1} versus the peak at 1410 cm^{-1} of the in-plane deformation of the benzene ring, which is usually considered as an internal standard in PET infrared spectroscopy studies [41,42]. **Fig. 4a** shows the evolution of both signals A_{1240}/A_{1410} and A_{3425}/A_{1410}. On the one hand, faster degradation was suggested by the greater variation of both indexes in the early stages of immersion below 30 min, which slowed down at higher immersion times. This observation is in line with the previously reported asymptotic behaviour contribution of time and supports the selection of 30 min as a reasonable standard time for assessing the effects of temperature [55,56,62,63]. On the other hand, temperature revealed an opposite performance to time, with a low degradation rate below 170 °C and acceleration with a linear pattern above such temperature [56]. Again, the inflexion point at 180 °C motivates the selection of this temperature for evaluating the consequences of time. This is in line with other studies in the literature, which also selected 180 °C as the optimal temperature for the glycolysis of PET in non-catalysed glycolysis [28].

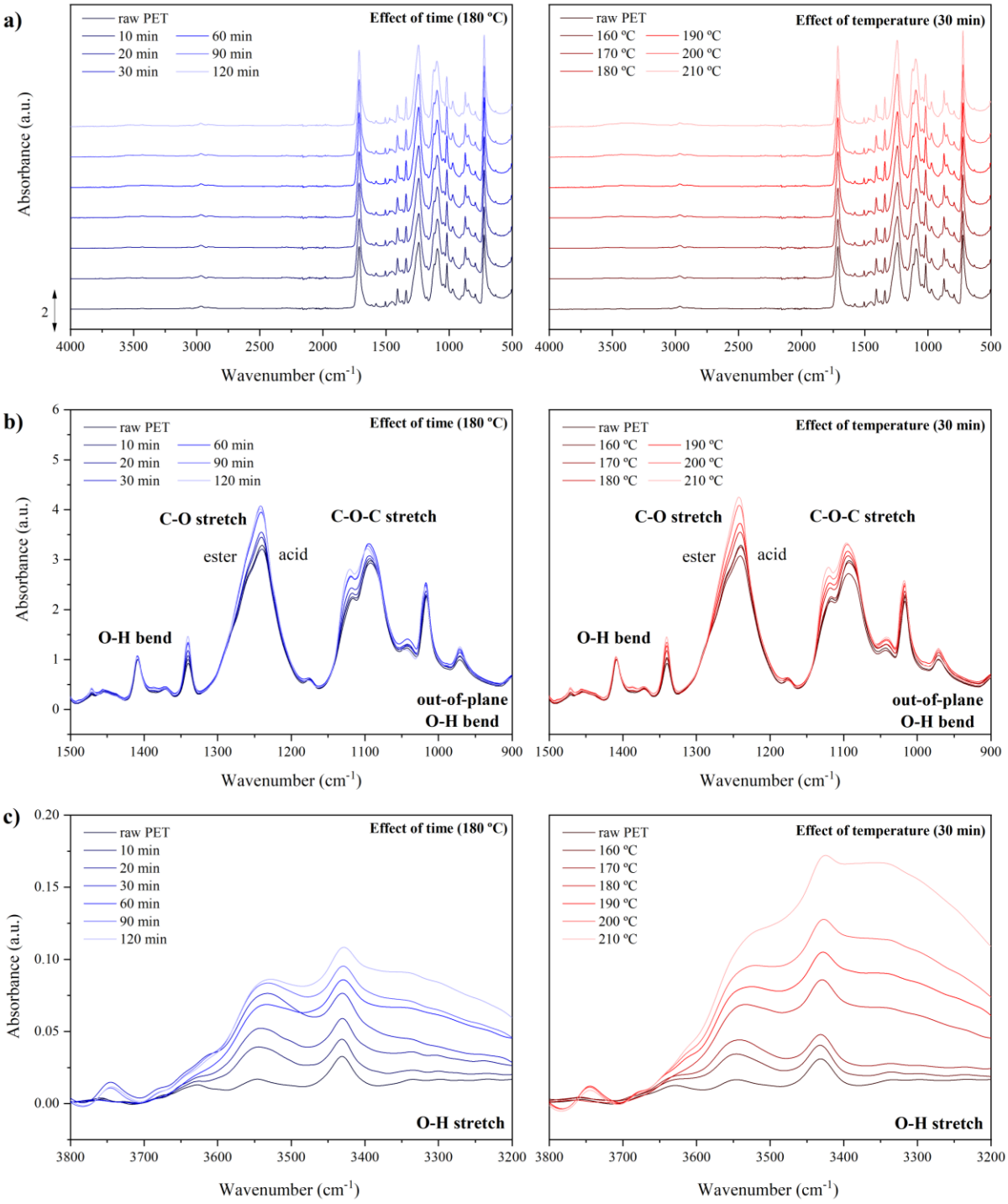

Fig. 3. (**a**) FT-IR spectra in the wavenumber range of 4000 to 400 cm^{-1}; (**b**) Hydroxyl and carbonyl region; and (**c**) O-H stretching bands as a function of time (left) and temperature (right) of glycolysis.

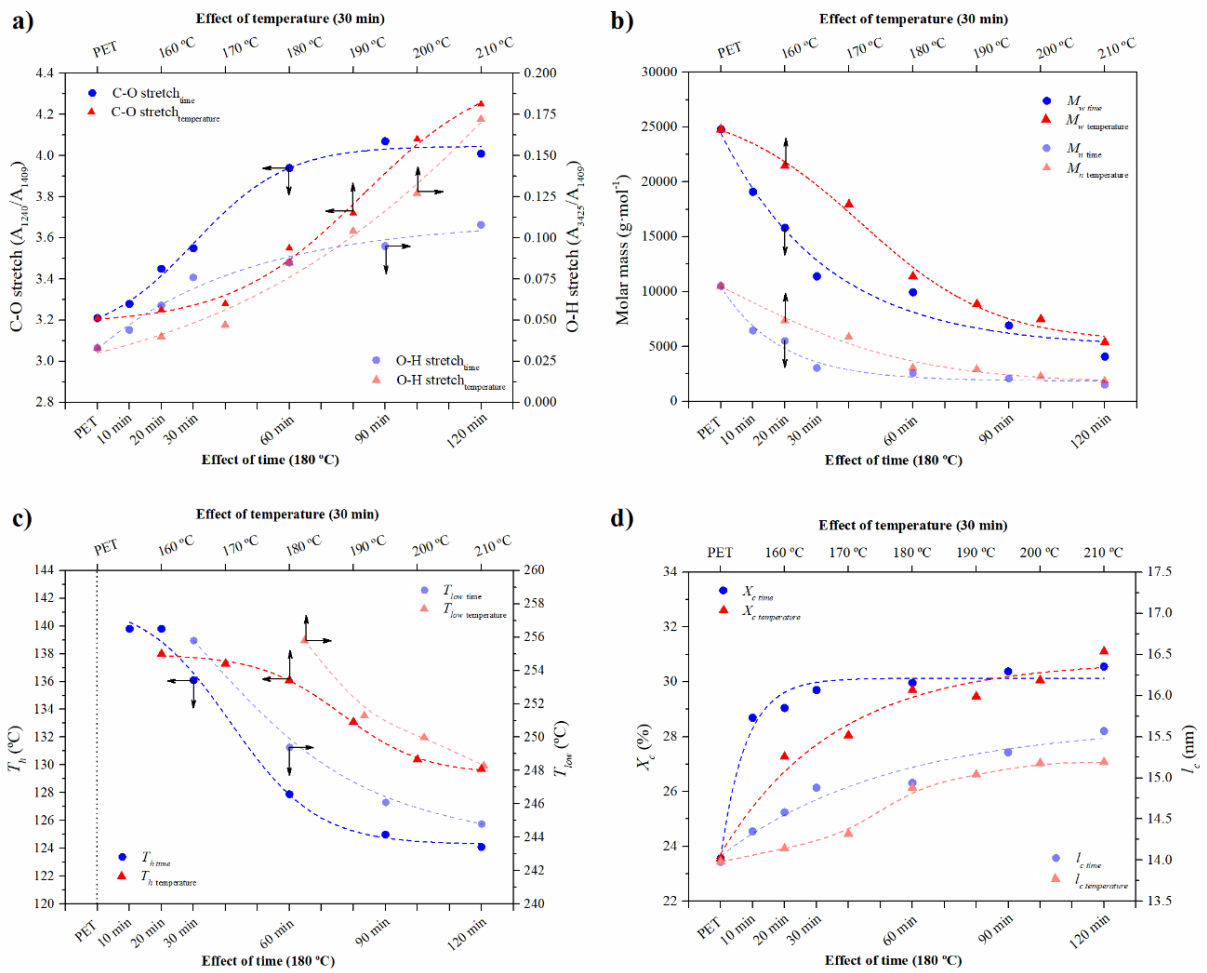

Fig. 4. Selected indicators as a function of time and temperature of glycolysis: (**a**) Normalised absorbance of the C–O and O–H stretching signals at 1240 and 3425 cm^{-1} versus the peak at 1410 cm^{-1} of the in-plane deformation of the benzene ring; (**b**) Average molar mass in number (M_n) and average molar mass in weight (M_w); (**c**) Peak temperatures of humidity release (T_h) and decomposition of low molar mass compounds (T_{low}); (**d**) Crystallinity degree (X_c) and lamellar thickness (l_c). Standard deviation was omitted for the sake of clarity.

3.3. Molar mass affectation during glycolysis

Due to the glycolytic process, PET chain scission and transesterification reactions with ethylene glycol may promote a length reduction of the macromolecules. The molar mass distributions shown in **Fig. 5** reveal that longer immersion time and higher temperatures displaced the Gaussian distributions towards lower values, with slightly different performances. While the immersion time promoted dissimilarities among the size of the PET macromolecules, related to an increment of the polydispersity index, higher temperatures kept the original shape unaltered, representing minor changes in polydispersity.

Particular allusion must be given to the low molar mass cue shown in all cases from the early stages of immersion, already found by other authors during the glycolysis of PET [29,57]. This small peak at low temperatures and low immersion time, which appeared as a shoulder when glycolytic conditions were emphasised, was located between molar mass values from 100 to 1000 g·mol^{-1}. Considering the molar mass of BHET ~254 g·mol^{-1}, this low molar mass population would be ascribed to BHET molecules, dimers and trimers, as observed in the inset of **Fig. 5**.

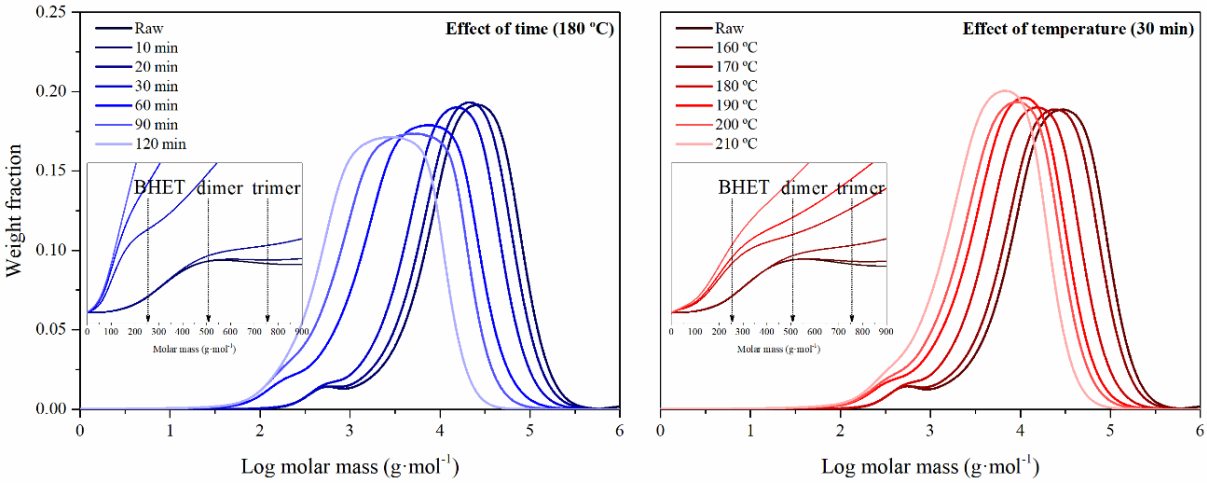

Fig. 5. Molar mass distributions as a function of time (left) and temperature (right) of glycolysis.

Given the virtual retention of the initial PET mass in the solid phase during glycolysis, and although the generation of low molar mass compounds was at this time demonstrated, it can be deduced that these small molecules have been retained in the bulk of PET particles, in line with the spectroscopic results shown in the previous section. This is also aligned with the reported bulk degradation process for PET, with rapid diffusion of the liquid ethylene glycol into the solid phase, which causes random chain scission with subsequent reduction in the molar mass and intrinsic viscosity while mainly maintaining the mass of this solid phase, as schematised in **Fig. 1** [29].

The average molar mass in number (M_n) and weight (M_w) were calculated from the molar mass distributions. **Fig. 4b** represents M_n and M_w's evolution as a function of time and temperature. Both M_n and M_w showed a more accentuated decrease in the early stages of immersion and at low temperatures, followed by a slower reduction when time or temperature increased. These results align with other studies of PET glycolysis, where a fast chain scission was found in the early stages or lower temperatures, followed by a slower degradation process once the conditions with the maximum degradation rate were exceeded [55]. Altogether, the inflexion

points in the M_w and M_n evolution were situated at 30 min and 180 °C, and behaviours tended to resemble at higher temperatures. These findings support the close relation of time and temperature for the chain scission of PET, as it has been reported for polyesters above their glass transition temperature [64,65].

Altogether, even considering that the obtained M_n values are approximated and strictly correlated to the previous calibration procedure, it can be established that oligoesters with terminal and internal hydroxyl groups were generated during glycolysis with a number average degree of polymerisation ranging from ~54 units of the raw PET to ~8 units when studying the influence of time, and to ~10 units when assessing the effect of temperature. Other authors found glycolysed PET molecules with comparable polymerisation degrees (5 to 40 units), and have applied them in the solid-state polycondensation of pre-polymers. Pre-polymers with such polymerisation degrees were pointedly faster than the standard process, allowing for obtaining higher molecular weights of PET without requiring an intermediate polymerisation step in solution [35–37]. Analogously, the glycolysis products generated in this work would be valuable candidates for being used as pre-polymers for reaching high molar mass and fast polymerisation processes of PET.

3.4. Thermo-oxidative behaviour of glycolysed PET

Thermogravimetric analyses in an oxidative atmosphere allowed for a complimentary evaluation of the glycolytic process of PET. **Fig. 6** shows the thermogravimetric (TG) and first derivative (DTG) curves as a function of time and temperature, which were examined in detail to obtain several indicators. The onset temperature (T_{onset}) was gained from the TG curves, while the DTG traces provided the peak temperatures of the different processes (T_h, T_{low}, T_{peak}).

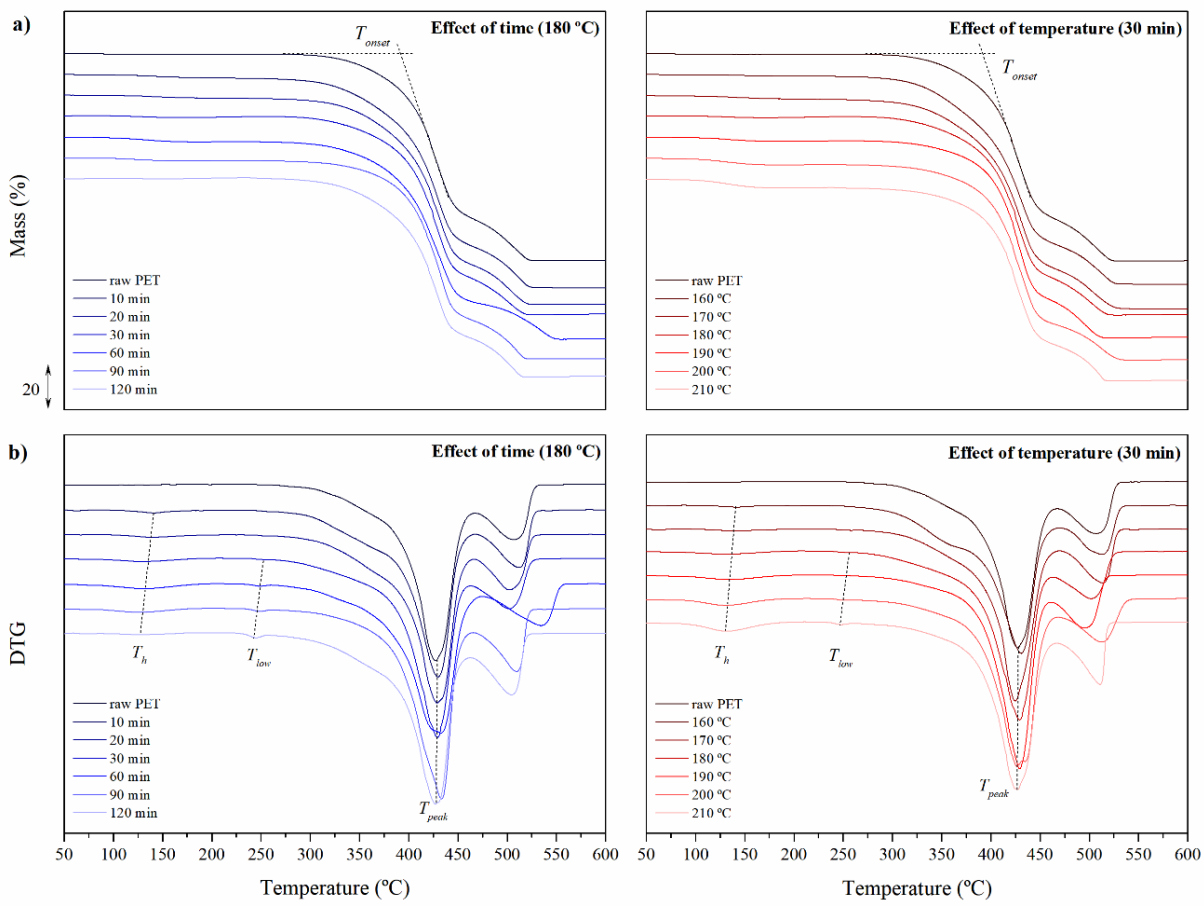

Fig. 6. (**a**) Thermogravimetric; and (**b**) derivative thermogravimetric curves (DTG) as a function of time (left) and temperature (right) of glycolysis.

Raw PET showed the typical decomposition profile in a single main stage in the range from 295 to 455 °C with an onset (T_{onset}) of 401 °C, a mass loss of nearly 80% and a peak temperature (T_{peak}) at 428 °C [66]. At higher temperatures, a stage for char decomposition was observed above 470 °C, with a peak temperature of around 510 °C and a mass contribution of about 20%. As expected, complete virtual decomposition of PET was achieved, with a solid residue at the end of the assay lower than 1%. These mass loss stages are correlated to the thermal decomposition mechanism of PET, which involves intramolecular back-biting, leading to cyclic dimers or trimers, and via chain scission leading to vinyl ester and acid end-groups [67,68].

Once exposed to glycolytic conditions, two small stages with peaks in the DTG curves at around 140 and 250 °C were perceived, which were absent in the raw PET. These peaks, which temperatures were labelled as T_h and T_{low} and are plotted in **Fig. 4c**, can be ascribed to the release of humidity moieties and the subsequent vaporisation of glycolysed low molar mass compounds, respectively.

The structural changes in the PET during glycolysis have been found to imply a more hydrophilic structure due to the presence of more hydroxyl groups, as revealed by spectroscopic analyses. Such functional groups allow for more significant interactions with water molecules from the rinsing stage and ambient humidity during management and storage. Indeed, the humidity percentage increased as a function of glycolysis time (from 1.2 to 2.7%) and temperature (from 0.9 to 4.4%), while the humidity release temperature (T_h) relevantly decreased during immersion. Nevertheless, the values of T_h greater than 125 °C in all cases demonstrated that water molecules were bound to the hydrophilic PET-based segments.

It has been reported that the thermal decomposition of BHET and small oligomers involves a first mass loss stage (30 to 50%) during heating around 250 °C, followed by the second mass loss (70 to 50%) around 450 °C [62,69]. Therefore, the peak labelled as T_{low} demonstrated the presence of low molar mass molecules involving short molecules with one or two units. The second stage at 450 °C coincides with that identified for PET and is due to the thermal repolymerisation of BHET during the heating program of TGA, with the subsequent elimination of hydroxyl formic acid ester [70,71]. Complimentary to the previous spectroscopic and chromatographic results, the presence of oligomers in this study was identified as a small peak in the DTG curves for glycolysed PET above 20 min of immersion and at 180 °C and higher temperatures. This peak moved towards lower temperatures as glycolysis time and temperature increased, thus demonstrating the generation of shorter molecules during more severe conditions.

The onset (T_{onset}) and peak (T_{peak}) temperatures for the main thermo-oxidative decomposition stage of PET are gathered in **Table 1**. After being subjected to the mildest glycolysis conditions, the onset (T_{onset}) decreased and was followed by a progressive increase for higher immersion times and temperatures. This phenomenon could be visually perceived in the DTG curves as a shoulder preceding the main peak and can be ascribed to partially glycolysed PET macromolecules [55]. It has been reported that the thermal decomposition of PET is enhanced by the presence of aliphatic end-groups [72], remnant humidity [73], and mainly due to the presence of ethylene glycol moieties [74]. Although at the mildest glycolysis conditions, oligomeric molecules from PET were still not generated, partially degraded polymer chains with ethylene glycol units and interacting with water molecules were produced, as demonstrated by this shoulder overlapped to the primary decomposition step of PET, and reported for glycolysis reactions in the absence of catalyst [59]. As the glycolysis conditions were more severe, degradation advanced, and such partially broken molecules turned into molecules with

one, two or three units, counterbalancing the presence of this shoulder with the peak mentioned above for low molar mass compounds. The peak temperature (T_{peak}) of the principal stage remained virtually unaltered during glycolysis, regardless of time and temperature conditions. Although this is often considered a sign of stability, chain scission was previously demonstrated by decreased molar mass and the generation of termination hydroxyl functional groups. In this case, it can be said that PET macromolecules' perceived molar mass reduction was not critical enough for displacing the main decomposition stage towards lower temperatures.

From a technological perspective, despite the severe molar mass reduction found in previous sections and considering the typical processing temperatures of PET in the range from 265 to 280 °C [75], the calculated T_{onset} and T_{peak} values above these temperatures suggest that glycolysed PET could be processed applying comparable temperature programs to those for raw PET. Nevertheless, to avoid processing issues caused by the presence of remnant water molecules (1-5%) that can cause hydrolytic reactions of PET during heating, glycolysed powder would require a proper drying stage to reach moisture presence below 0.02% before being reprocessed [76].

3.5. Thermal properties and crystalline morphology of glycolysed PET

The thermal properties and crystalline morphology were calorimetrically evaluated during glycolysis. The samples were subjected to successive heating/cooling/heating segments with which the thermal history was removed, and a controlled crystalline structure was promoted. The calorimetric thermograms for the cooling and second heating segments are plotted in **Fig. 7a** and **7b**, respectively. From the cooling segment, the glass transition temperatures (T_g) and crystallisation temperature and enthalpy (T_c) were obtained, while the second heating provided the values of the melting temperature and enthalpy (T_m), all of them gathered in **Table 1**. The degree of crystallinity (X_c) was calculated from the melting enthalpy with **Eq. 2**, and plotted in **Fig. 4d**, together with the lamellar thickness (l_c) obtained with **Eq. 3** as a function of glycolysis time and temperature.

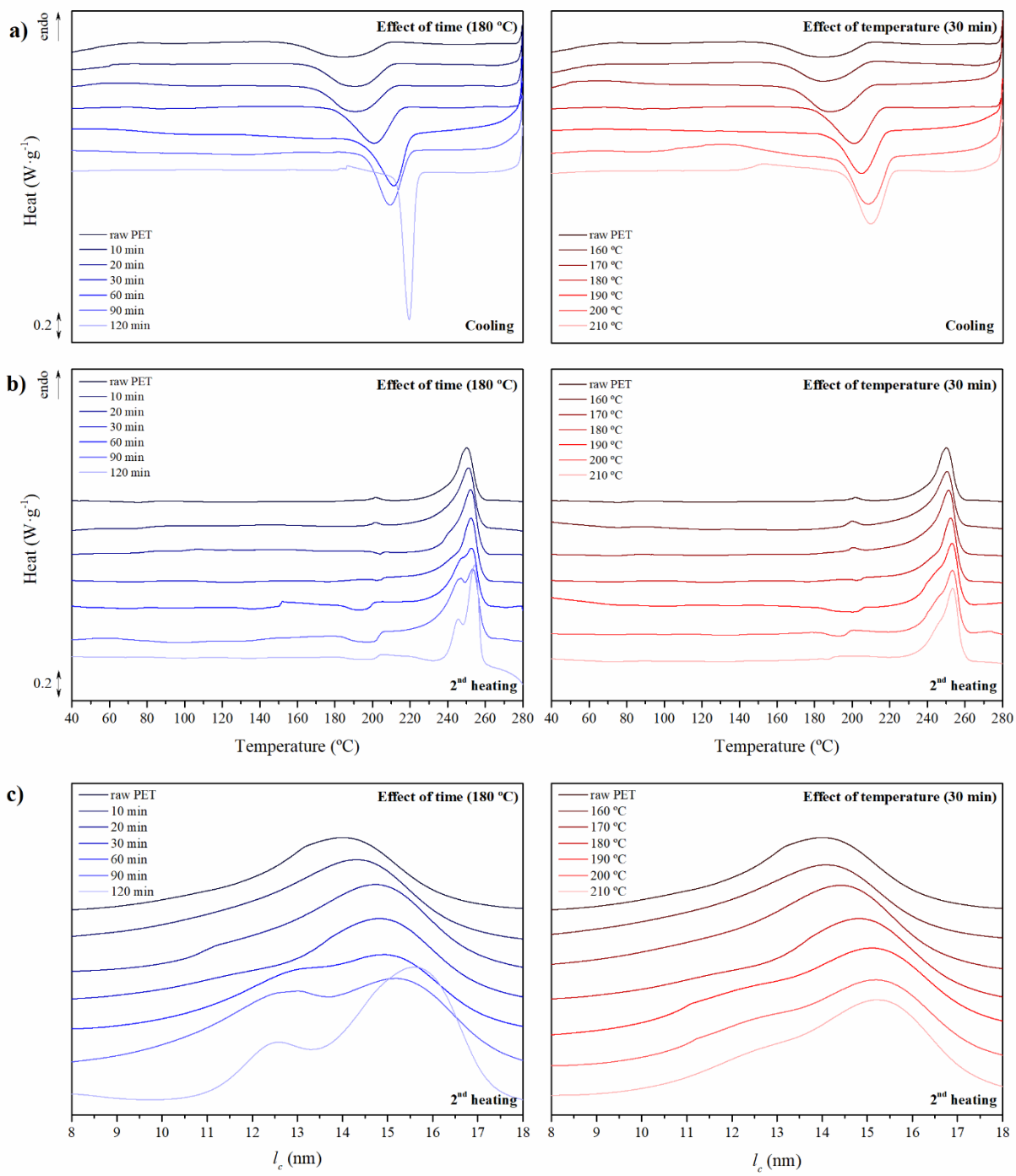

Fig. 7. (**a**) Calorimetric thermograms for the cooling; (**b**) second heating scan; and (**c**) lamellar thickness (l_c) distributions as a function of time (left) and temperature (right) of glycolysis.

The glass transition of PET was identified in the vicinities of 85 °C during cooling, while the crystallisation was manifested in a broad exothermic process with a peak temperature of 185 °C. The endothermic melting transition during heating was visualised as the primary peak around 250 °C, representing an X_c of 26%, in line with previous reports for semicrystalline PET [77,78]. Complementarily, a minor melting event was found around 200 °C, correlated to

imperfect crystalline domains composed of oligomeric species of PET that melted at low temperatures. Similar secondary melting transitions have been reported during thermo-oxidative ageing of PET [79] or after several reprocessing cycles [78]. Other studies found comparable melting points of oligomeric species of PET with an equivalent degree of polymerisation as those in this work [80].

The glycolytic treatment promoted lower glass transition temperatures, sharper and larger crystallisation during cooling occurring at higher temperatures, melting in a multimodal fashion and more crystallinity. All these signs are characteristic features of polymer degradation and corroborate the chain scission phenomena revealed by the molar mass analyses. This chain breakage occurs preferentially in the amorphous domains [81]. Shorter polymer chains after glycolytic scission possess lower glass transition temperature and greater mobility as the glycolysis progresses and can rearrange and form more crystalline domains at higher temperatures during cooling [29].

Particularly for the crystalline structure, **Fig. 4d** shows that X_c sharply increased from 26 to 29% after 10 min of immersion, and then it progressively increased to 31% after 20, 30, 60 and 120 min. The l_c regularly rose from 13.9 to 15.5 nm with immersion time. In terms of glycolysis temperature, a more gradual increase of X_c was observed, reaching 31% after immersion at 210 °C. l_c was scarcely affected at 160 °C, remaining around 14.1 nm, and then it 7 increased to 15.2 nm for the most severe temperatures.

The lamellar thickness distributions were comprehensively studied from the melting peaks to elucidate the changes in the crystalline morphology during glycolysis. The Thomson-Gibbs equation (**Eq. 3**) was applied, considering the Hoffman-Lauritzen nucleation theory [44–46]. **Fig. 7c** shows the l_c distributions for raw and glycolysed PET as a function of time and temperature, where the distribution related to the most probable lamellar size can be appreciated, showing a multimodal performance. The presence of multiple peaks can be ascribed to the coexistence of different crystalline populations [82–84], which were studied in detail with a two-gaussian peak deconvolution approach using the Origin software and the Levenberg Marquardt iteration algorithm [85,86]. Sub-peaks were labelled as populations I and II from lower to higher l_c. Therefore, the melting temperatures (T_{mI} and T_{mII}) and the crystallinity degrees (X_{cI} and X_{cII}) for both crystalline populations I and II could be approximated. Moreover, considering a partial areas study, its contribution to the overall crystallinity was estimated (X^I

and X^{II}) [78,85]. All these values are gathered in **Table 1** as a function of the glycolysis time and temperature.

The lamellar thickness of both populations I and II increased after all the glycolysis treatments, more the longer time and greater temperature of immersion, as revealed by the higher melting temperatures (T_{mI} and T_{mII}). If the partial contribution of the populations is considered (X^I and X^{II}), the initial prevalence of population II generally turned into a more balanced proportion with population I for more severe glycolysis conditions. Particularly for the effect of immersion time, the contribution of the population I progressively gained importance up to 60 and 90 min from ~14% to ~53%. From 90 min onwards, the proportions of the crystalline domains of both populations were almost identical. The change in the tendency at 120 min, where the percentage of population I significantly decreased to values close to ~24%, can be ascribed to the glycolytic attack of crystalline domains of population I, with lower lamellar thickness and more labile to degradation than population II [29]. With higher temperatures, a slightly smothered performance was found. The contribution of the population I increased from ~14% to ~35% after glycolysis at 190 °C. It gained importance for higher temperatures such as 200 and 210 °C and increased to values above ~42%. Overall, the exhaustive evaluation of the lamellar thickness of the different crystalline populations emphasised the prevalent degradation of the crystalline population with lower lamellar thickness and highlighted the more severe influence of the glycolysis time than that of temperature in the selected system.

Finally, it is interesting to note that, although previous results revealed the presence of BHET-based molecules and oligomers, the melting peaks of BHET and dimer/oligomers generated during glycolytic reactions reported in the literature at ~110 and ~170 °C, respectively, were absent in the thermograms regardless of immersion time and temperature [55,59,61,62,69,87,88]. This observation has already been reported in studies dealing with non-catalysed glycolysis of PET at 196 °C [26] or in sodium carbonate-catalysed glycolysis at this temperature up to 120 min [57]. Altogether, considering the indications of spectroscopic, molar mass and thermogravimetric analyses, it can be suggested that the glycolysed low molar mass species were spatially confined into the PET particles, with the subsequent molecular environment composed of longer polymer chains that prevented small glycolysed molecules from crystallising and having their own melting peak during the heating calorimetric scan.

Table 1. Onset (T_{onset}) and peak (T_{peak}) temperatures for the main stage of thermo-oxidative decomposition; glass transition temperature (T_g), crystallisation temperature (T_c), and adjusted melting temperatures (T_{mI} and T_{mII}) and crystallinity degree (X_{cI} and X_{cII}) together with the partial contribution (X_I and X_{II}) of the different crystalline populations (I and II) as a function of the time and temperature of glycolysis.

	T_{onset} (°C)	T_{peak} (°C)	T_g (°C)	T_c (°C)	Population I			Population II		
					T_{mI} (°C)	X_{cI} (%)	X^I (%)	T_{mII} (°C)	X_{cII} (%)	X^{II} (%)
PET	401.0	426.9	85.3	184.7	239.3	3.4	14.3	250.1	20.2	85.7
10 min	388.9	431.0	79.3	188.6	242.3	8.9	30.6	251.2	20.2	69.4
20 min	385.5	430.1	82.5	194.2	243.9	7.4	26.9	252.3	20.0	73.1
30 min	388.5	432.0	79.7	202.5	244.8	10.5	35.4	252.8	19.2	64.6
60 min	388.8	433.7	80.9	211.5	246.3	15.1	50.4	253.3	14.9	49.6
90 min	394.4	431.8	78.6	211.8	245.4	17.0	52.8	253.8	15.2	47.2
120 min	396.4	424.6	79.0	219.6	245.7	7.4	24.1	254.0	23.2	75.9
160 °C	384.3	430.4	80.2	183.6	242.5	10.7	36.8	250.8	18.4	63.2
170 °C	383.9	427.9	80.0	190.3	243.6	10.3	37.7	251.6	17.0	62.3
180 °C	388.5	432.0	79.7	202.5	244.8	10.5	35.4	252.8	19.2	64.6
190 °C	396.9	427.8	79.1	205.2	244.1	9.9	33.1	253.4	20.0	66.9
200 °C	399.7	422.3	73.5	208.9	245.8	12.7	39.6	253.8	19.4	60.4
210 °C	397.4	425.7	-	209.8	247.1	13.0	42.6	254.0	17.5	57.4

3.6. Modelling physico-chemical properties as a function of glycolysis time and temperature

Previous sections demonstrated that the physico-chemical properties of PET meaningfully vary during the heterogeneous glycolytic process that lately coexists with a minor homogeneous stage. Significant changes have been found in the chemical structure, molar mass, thermo-oxidative stability and crystalline structure when applying different time and temperature glycolysis conditions.

Polymer materials like PET require specific physico-chemical performance for particular applications, given by precise chain lengths, functional groups or crystalline morphology. Indeed, correlating the structure and application behaviour of PET has been the focus of numerous studies in the literature. For instance, the crystalline morphology has been associated with the mechanical properties in films, injection moulded preforms and stretching-blown bottles with distinct blowing conditions [89]. Also, the structure and properties of PET-based fibres [90,91] and crystallised, annealed and quenched PET [92] have been studied. Results revealed that the elastic modulus is determined by the mobility of the amorphous phase and its level of molecular orientation. Greater mobility and lower orientation lead to less rigid specimens, which are also closely linked to molar mass [75]. Low-molar mass polymers possess higher flexibility than those with high-molar mass. The more significant molecular

entanglements in high-molar mass structures restrain uncoiling under external mechanical stimuli and reduce flexibility. In this regard, the existence of chemical interactions together with the presence of polar groups may limit their mobility and promote the kinetic rigidity of the polymer chains. Similar studies were carried out with recycled PET, where the role of crystalline, mobile amorphous and rigid amorphous fractions in its performance was elucidated [85]. Degradation caused by reprocessing cleaved mobile amorphous fractions and shortened PET chains. These smaller molecules reorganised into rigid amorphous fractions and formed crystalline domains of smaller lamellar thickness. Consequently, reprocessing reduced the stress and elongation at break, given the more brittle materials with lower ductility.

Therefore, modelling the change of physico-chemical properties of given solid fractions of PET waste as a function of glycolysis conditions may be highly relevant for tailoring their performance. Here, mathematical correlations of the assessed physico-chemical indicators are proposed as a valuable strategy for predicting the performance of glycolysed PET in this particular system. **Table 2** gathers the proposed empirical equations for the studied parameters, as plotted in **Fig. 4**. The changes in the absorbance of carbonyl (A_{1240}) and hydroxyl signals (A_{3425}), the average molar mass in number (M_n) and weight (M_w), the humidity release temperature (T_h), the crystallinity degree (X_c) and the lamellar thickness (l_c) were all fitted to a Boltzmann function. In general, fittings revealed adjusted R^2 above 0.95, which indicates that more than 95% of the output variables variation for this particular system is explained by the input variables, i.e. time and temperature, allowing for a successful prediction of the glycolytic performance.

Table 2. Mathematical equations modelling the variation of chemical structure, molar mass, thermo-oxidative decomposition and crystalline morphology.

	As a function of temperature	As a function of time
Normalised absorbance C–O stretching (A_{1240})	$A_{1240}(T) = 4.4 - \frac{1.3}{1 + e^{\frac{T-191.5}{10.3}}}$ $R^2 = 0.98$	$A_{1240}(t) = 4.0 - \frac{0.9}{1 + e^{\frac{t-30.3}{14.4}}}$ $R^2 = 0.99$
Normalised absorbance O–H stretching (A_{3425})	$A_{3425}(T) = 0.5 - \frac{0.5}{1 + e^{\frac{T-231.5}{28.6}}}$ $R^2 = 0.97$	$A_{3425}(t) = 0.1 - \frac{61.2}{1 + e^{\frac{t+313.4}{47.0}}}$ $R^2 = 0.96$
Average molar mass in number (M_n)	$M_n(T) = 1.7 \cdot 10^3 + \frac{1.6 \cdot 10^4}{1 + e^{\frac{T+152.5}{14.0}}}$ $R^2 = 0.97$	$M_n(t) = 1.8 \cdot 10^3 + \frac{3.0 \cdot 10^7}{1 + e^{\frac{t+153.5}{18.8}}}$ $R^2 = 0.96$
Average molar mass in weight (M_w)	$M_w(T) = 5.7 \cdot 10^3 + \frac{1.9 \cdot 10^4}{1 + e^{\frac{T-173.5}{9.2}}}$ $R^2 = 0.99$	$M_w(t) = 4.5 \cdot 10^3 + \frac{1.5 \cdot 10^8}{1 + e^{\frac{T+331.9}{36.9}}}$ $R^2 = 0.95$
Humidity release temperature (T_h)	$T_h(T) = 129.9 + \frac{8.6}{1 + e^{\frac{T-188.1}{6.4}}}$ $R^2 = 1.00$	$T_h(t) = 124.3 + \frac{17.5}{1 + e^{\frac{t-41.6}{13.5}}}$ $R^2 = 0.99$
Crystallinity degree (X_c)	$X_c(T) = 30.8 - \frac{9.5 \cdot 10^4}{1 + e^{\frac{T+21.7}{18.1}}}$ $R^2 = 0.95$	$X_c(t) = 30.1 - \frac{1.1 \cdot 10^5}{1 + e^{\frac{t+76.7}{7.9}}}$ $R^2 = 0.95$
Lamellar thickness (l_c)	$l_c(T) = 15.2 - \frac{1.2}{1 + e^{\frac{T-174.7}{6}}}$ $R^2 = 0.99$	$l_c(t) = 15.7 - \frac{8.5 \cdot 10^3}{1 + e^{\frac{t+460.7}{53.7}}}$ $R^2 = 0.95$

Altogether, it can be understood that modelling the consequences of glycolytic treatment, which promoted an increase in polar groups, reduced molar mass and increased crystallinity of PET, is of high significance for further application of the obtained glycolysed PET fractions. In addition to these intrinsic features of PET given by glycolysis, the effect of processing conditions [75], i.e. temperature program and orientation, on the crystallisation rate may be highlighted, which are of crucial relevance for promoting particular morphologies and performance that meet the application demands.

4. Conclusions

The glycolysis of PET in the considered times (10 to 120 min at 180 °C) and temperatures (160 to 210 °C during 30 min) involved a heterogeneous process concerning the diffusion of ethylene glycol (EG) into the bulk solid PET pellets and attack of amorphous regions, lately coexisting with the beginning of the homogeneous stage with the further generation of oligomers and a minor number of BHET molecules. Although significant chain scission was encountered, the

initial mass of the solid fraction remained virtually constant with separated solid and liquid phases.

Monitoring the glycolysis process in the solid fraction of PET allowed the demonstration of simultaneous bulk and surface degradation processes. Degradation was complementarily identified by an increase in the proportion of polar hydroxyl groups, a significant molar mass reduction, and the generation of a low-lamellar thickness crystalline population. The empirical evaluation of these changes, all of them following a Boltzmann equation, offers the possibility of establishing mathematical correlations for predicting and tailoring the physico-chemical performance of PET on demand as a function of glycolysis time and temperature. For this particular system, it can be emphasised that even though an asymptotic performance was found in both factors, the increase in the glycolysis time promoted more severe consequences than the temperature variation.

According to their glycolysis degree, the obtained glycolysed fractions of PET waste can be considered appropriate for closed-loop, semi-closed, and open-loop chemical recycling, with different applications of varying values through a simple, green, and versatile process. Hence, incorporating glycolysis into PET recycling practices not only mitigates potential drawbacks linked to alternative processes but also opens up opportunities for a more diverse range of end-product applications. A comprehensive approach, encompassing chemical, mechanical, and complementary strategies, ensures a more holistic and effective strategy for the sustainable valorisation of PET.

Acknowledgements

The authors would like to thank the support of the Generalitat Valenciana for the APOSTD/2020/155 contract for O. Gil-Castell.

Declarations

Competing interests

The authors disclose non-financial interests that are directly or indirectly related to the present work.

Data availability

The datasets generated during and/or analysed during the current study are available from the corresponding author upon reasonable request.

Author contributions

Conceptualization: S. Llopis, O. Gil-Castell, E. Verdejo, A. Ribes-Greus; Methodology: S. Llopis, O. Gil-Castell; Formal analysis and investigation: S. Llopis, O. Gil-Castell, E. Verdejo, A. Ribes-Greus; Writing - original draft preparation: S. Llopis, O. Gil-Castell; Writing - review and editing: S. Llopis, O. Gil-Castell, E. Verdejo, A. Ribes-Greus; Funding acquisition: E. Verdejo, A. Ribes-Greus; Resources: E. Verdejo, A. Ribes-Greus; Supervision: E. Verdejo, A. Ribes-Greus

References

[1] Plastics Europe, Plastics – the Facts 2022, (2022). https://plasticseurope.org/knowledge-hub/plastics-the-facts-2022/.

[2] R. Nisticò, Polyethylene terephthalate (PET) in the packaging industry, Polym Test. 90 (2020) 106707. https://doi.org/10.1016/J.POLYMERTESTING.2020.106707.

[3] V. Kouloumpis, R.S. Pell, M.E. Correa-Cano, X. Yan, Potential trade-offs between eliminating plastics and mitigating climate change: An LCA perspective on Polyethylene Terephthalate (PET) bottles in Cornwall, Science of The Total Environment. 727 (2020) 138681. https://doi.org/10.1016/J.SCITOTENV.2020.138681.

[4] M. Rybaczewska-Blazejowska, A. Mena-Nieto, Circular economy: comparative life cycle assessment of fossil polyethylene terephthalate (PET) and its recycled and bio-based counterparts, Management and Production Engineering Review. Vol. 11, No. 4 (2020) 121–128. https://doi.org/10.24425/MPER.2020.136126.

[5] R.P. Magalhães, J.M. Cunha, S.F. Sousa, Perspectives on the role of enzymatic biocatalysis for the degradation of plastic pet, Int J Mol Sci. 22 (2021) 11257. https://doi.org/10.3390/IJMS222011257/S1.

[6] L. Shi, L. Zhu, Recent Advances and Challenges in Enzymatic Depolymerization and Recycling of PET Wastes, ChemBioChem. (2023) e202300578. https://doi.org/10.1002/CBIC.202300578.

[7] B. Guo, X. Lopez-Lorenzo, Y. Fang, E. Bäckström, A.J. Capezza, S.R. Vanga, I. Furó, M. Hakkarainen, P.O. Syrén, Fast Depolymerization of PET Bottle Mediated by Microwave Pre-Treatment and An Engineered PETase**, ChemSusChem. 16 (2023) e202300742. https://doi.org/10.1002/CSSC.202300742.

[8] E. Bäckström, K. Odelius, M. Hakkarainen, Ultrafast microwave assisted recycling of PET to a family of functional precursors and materials, Eur Polym J. 151 (2021) 110441. https://doi.org/10.1016/J.EURPOLYMJ.2021.110441.

[9] J.Y. Jang, K. Sadeghi, J. Seo, Chain-Extending Modification for Value-Added Recycled PET: A Review, Polymer Reviews. 62 (2022) 860–889. https://doi.org/10.1080/15583724.2022.2033765.

[10] J. Zhou, T.G. Hsu, J. Wang, Mechanochemical Degradation and Recycling of Synthetic Polymers, Angewandte Chemie International Edition. 62 (2023) e202300768. https://doi.org/10.1002/ANIE.202300768.

[11] A.B. Raheem, Z.Z. Noor, A. Hassan, M.K. Abd Hamid, S.A. Samsudin, A.H. Sabeen, Current developments in chemical recycling of post-consumer polyethylene terephthalate wastes for new materials production: A review, J Clean Prod. 225 (2019) 1052–1064. https://doi.org/10.1016/j.jclepro.2019.04.019.

[12] S. Li, I. Cañete Vela, M. Järvinen, M. Seemann, Polyethylene terephthalate (PET) recycling via steam gasification – The effect of operating conditions on gas and tar composition, Waste Management. 130 (2021) 117–126. https://doi.org/10.1016/J.WASMAN.2021.05.023.

[13] A. El Mejjatti, T. Harit, A. Riahi, R. Khiari, I. Bouabdallah, F. Malek, Chemical recycling of poly(ethylene terephthalate). application to the synthesis of multiblock copolyesters, Express Polym Lett. 8 (2014) 544–553. https://doi.org/10.3144/expresspolymlett.2014.58.

[14] K. Ghosal, C. Nayak, Recent advances in chemical recycling of polyethylene terephthalate waste into value added products for sustainable coating solutions-hope vs. hype, Mater Adv. 3 (2022) 1974–1992. https://doi.org/10.1039/d1ma01112j.

[15] D.E. Nikles, M.S. Farahat, New motivation for the depolymerization products derived from poly(ethylene terephthalate) (PET) waste: A review, Macromol Mater Eng. 290 (2005) 13–30. https://doi.org/10.1002/mame.200400186.

[16] V. Sinha, M.R. Patel, J. V. Patel, PET Waste Management by Chemical Recycling: A Review, J Polym Environ. 18 (2010) 8–25. https://doi.org/10.1007/s10924-008-0106-7.

[17] A. Singh, S.L. Banerjee, K. Kumari, P.P. Kundu, Recent Innovations in Chemical Recycling of Polyethylene Terephthalate Waste: A Circular Economy Approach Toward Sustainability, in: Handbook of Solid Waste Management, 2022: pp. 1149–1176. https://doi.org/10.1007/978-981-16-4230-2_53.

[18] J. Xin, Q. Zhang, J. Huang, R. Huang, Q.Z. Jaffery, D. Yan, Q. Zhou, J. Xu, X. Lu, Progress in the catalytic glycolysis of polyethylene terephthalate, J Environ Manage. 296 (2021) 113267. https://doi.org/10.1016/j.jenvman.2021.113267.

[19] A. Sheel, D. Pant, Chemical Depolymerization of PET Bottles via Glycolysis, in: Recycling of Polyethylene Terephthalate Bottles, William Andrew Publishing, 2019: pp. 61–84. https://doi.org/10.1016/b978-0-12-811361-5.00004-3.

[20] Z. Guo, E. Adolfsson, P.L. Tam, Nanostructured micro particles as a low-cost and sustainable catalyst in the recycling of PET fiber waste by the glycolysis method, Waste Management. 126 (2021) 559–566. https://doi.org/10.1016/J.WASMAN.2021.03.049.

[21] N. Wagner, L. Wen, C.J.R. Frazão, T. Walther, Next-generation feedstocks methanol and ethylene glycol and their potential in industrial biotechnology, Biotechnol Adv. 69 (2023) 108276. https://doi.org/10.1016/J.BIOTECHADV.2023.108276.

[22] G.W. Huber, S. Iborra, A. Corma, Synthesis of transportation fuels from biomass: Chemistry, catalysts, and engineering, Chem Rev. 106 (2006) 4044–4098. https://doi.org/10.1021/CR068360D/ASSET/IMAGES/MEDIUM/CR068360DF00035.GIF.

[23] H. Yue, Y. Zhao, X. Ma, J. Gong, Ethylene glycol: properties, synthesis, and applications, Chem Soc Rev. 41 (2012) 4218–4244. https://doi.org/10.1039/C2CS15359A.

[24] F. Hubert, G. Durand, G. Tersac, Equilibria in the alcoholysis reactions of terephthalic esters and chemical valorization of polyethyleneterephthalate waste. I. Equilibrium constants determination, J Appl Polym Sci. 72 (1999) 329–340. https://doi.org/10.1002/(SICI)1097-4628(19990418)72:3<329::AID-APP3>3.0.CO;2-V.

[25] D. -C Wang, L. -W Chen, W. -Y Chiu, Kinetic study on depolymerization by glycolysis of poly(ethylene terephthalate) with bisphenol A, Die Angewandte Makromolekulare Chemie. 230 (1995) 47–71. https://doi.org/10.1002/APMC.1995.052300103.

[26] R. López-Fonseca, I. Duque-Ingunza, B. de Rivas, S. Arnaiz, J.I. Gutiérrez-Ortiz, Chemical recycling of post-consumer PET wastes by glycolysis in the presence of metal salts, Polym Degrad Stab. 95 (2010) 1022–1028. https://doi.org/10.1016/J.POLYMDEGRADSTAB.2010.03.007.

[27] J.R. Campanelli, M.R. Kamal, D.G. Cooper, Kinetics of glycolysis of poly(ethylene terephthalate) melts, J Appl Polym Sci. 54 (1994) 1731–1740. https://doi.org/10.1002/APP.1994.070541115.

[28] S. Katoch, V. Sharma, P.P. Kundu, M.B. Bera, Optimization of PET Glycolysis Process by Response Surface Methodological Approach: A Two-Component Modelling Using Glycolysis Time and Temperature, ISRN Polymer Science. 2012 (2012) 1–9. https://doi.org/10.5402/2012/630642.

[29] F. Pardal, G. Tersac, Kinetics of poly(ethylene terephthalate) glycolysis by diethylene glycol. I. Evolution of liquid and solid phases, Polym Degrad Stab. 91 (2006) 2840–2847. https://doi.org/10.1016/j.polymdegradstab.2006.09.009.

[30] A.K. Singh, R. Bedi, B.S. Kaith, Composite materials based on recycled polyethylene terephthalate and their properties – A comprehensive review, Compos B Eng. 219 (2021) 108928. https://doi.org/10.1016/J.COMPOSITESB.2021.108928.

[31] E.G. Ruiz, Y.-H.V. Soong, M.J. Sobkowicz, D. Xie, Recent Advances in Biological Recycling of Polyethylene Terephthalate (PET) Plastic Wastes, (2022). https://doi.org/10.3390/bioengineering9030098.

[32] M. Pu, X. Zhou, X. Liu, C. Fang, D. Wang, A facile, alternative and sustainable feedstock for transparent polyurethane elastomers from chemical recycling waste PET in high-efficient way, Waste Management. 155 (2023) 137–145. https://doi.org/10.1016/J.WASMAN.2022.10.032.

[33] M. Bedell, M. Brown, A. Kiziltas, D. Mielewski, S. Mukerjee, R. Tabor, A case for closed-loop recycling of post-consumer PET for automotive foams, Waste Management. 71 (2018) 97–108. https://doi.org/10.1016/J.WASMAN.2017.10.021.

[34] N.K. Bui, T. Satomi, H. Takahashi, Recycling woven plastic sack waste and PET bottle waste as fiber in recycled aggregate concrete: An experimental study, Waste Management. 78 (2018) 79–93. https://doi.org/10.1016/J.WASMAN.2018.05.035.

[35] B. Gantillon, R. Spitz, T.F. McKenna, The Solid State Postcondensation of PET, 2, Macromol Mater Eng. 289 (2004) 106–112. https://doi.org/10.1002/MAME.200300290.

[36] B. Gantillon, R. Spitz, T.F. McKenna, The Solid State Postcondensation of PET, 3, Macromol Mater Eng. 289 (2004) 113–118. https://doi.org/10.1002/MAME.200300291.

[37] B. Gantillon, R. Spitz, J.L. Lepage, T.F. McKenna, The Solid State Postcondensation of PET, 4, Macromol Mater Eng. 289 (2004) 119–130. https://doi.org/10.1002/MAME.200300292.

[38] D. Cevher, S. Sürdem, Polyurethane adhesive based on polyol monomers BHET and BHETA depolymerised from PET waste, Int J Adhes Adhes. 105 (2021) 102799. https://doi.org/10.1016/J.IJADHADH.2020.102799.

[39] P. Phuangngamphan, C. Thongpin, Synthesize of Polydiacetylene Containing Copolyurethane Using Polyol Product Derived from Chemical Recycling of PET Bottles, Energy Procedia. 56 (2014) 326–333. https://doi.org/10.1016/J.EGYPRO.2014.07.164.

[40] T. Sang, C.J. Wallis, G. Hill, G.J.P. Britovsek, Polyethylene terephthalate degradation under natural and accelerated weathering conditions, Eur Polym J. 136 (2020) 109873. https://doi.org/10.1016/j.eurpolymj.2020.109873.

[41] K.C. Cole, J. Guevremont, A. Ajji, M.M. Dumoulin, Characterization of surface orientation in poly(ethylene terephthalate) by front-surface reflection infrared spectroscopy, Appl Spectrosc. 48 (1994). https://doi.org/10.1366/0003702944027877.

[42] D.J. Walls, Application of ATR-IR to the Analysis of Surface Structure and Orientation in Uniaxially Drawn Poly(Ethyleneterephthalate), Appl Spectrosc. 45 (1991) 1193–1198. https://doi.org/10.1366/0003702914336147.

[43] B. Wunderlich, The Athas database on heat capacities of polymers, Pure and Applied Chemistry. 67 (1995) 1019–1026. https://doi.org/10.1351/PAC199567061019.

[44] J.I. Lauritzen, J.D. Hoffman, Formation of Polymer Crystals with Folded Chains from Dilute Solution, J Chem Phys. 31 (1959) 1680–1681. https://doi.org/10.1063/1.1730678.

[45] J.D. Hoffman, J.I. Lauritzen, Jr. John I. Lauritzen, Crystallization of Bulk Polymers With Chain Folding : Theory of Growth of Lamellar Spherulites, Journal of Research of the National Bureau of Standards - A. Physics and Chemistry. 65 (1961) 1961. https://doi.org/10.6028/jres.065A.035.

[46] J.D. Hoffman, G.T. Davis, J.I. Lauritzen, Crystalline and noncrystalline solids, New York, 1976. https://doi.org/10.1007/978-1-4684-2664-9.

[47] X.F. Lu, J.N. Hay, Isothermal crystallization kinetics and melting behaviour of poly(ethylene terephthalate), Polymer (Guildf). 42 (2001) 9423–9431. https://doi.org/10.1016/S0032-3861(01)00502-X.

[48] F. von Burkersroda, L. Schedl, A. Göpferich, A.G. F. von Burkersroda, L. Schedl, Why degradable polymers undergo surface erosion or bulk erosion, Biomaterials. 23 (2002) 4221–4231. https://doi.org/10.1016/S0142-9612(02)00170-9.

[49] D. Kint, S. Muñoz-Guerra, A review on the potential biodegradability of poly(ethylene terephthalate), (n.d.). https://doi.org/10.1002/(SICI)1097-0126(199905)48:5.

[50] T.B. Thomsen, K. Almdal, A.S. Meyer, Significance of poly(ethylene terephthalate) (PET) substrate crystallinity on enzymatic degradation, N Biotechnol. 78 (2023) 162–172. https://doi.org/10.1016/J.NBT.2023.11.001.

[51] S.S. Hosseini, S. Taheri, A. Zadhoush, A. Mehrabani-Zeinabad, Hydrolytic degradation of poly(ethylene terephthalate), J Appl Polym Sci. 103 (2007) 2304–2309. https://doi.org/10.1002/APP.24142.

[52] C. Sammon, J. Yarwood, N. Everall, An FT–IR study of the effect of hydrolytic degradation on the structure of thin PET films, Polym Degrad Stab. 67 (2000) 149–158. https://doi.org/10.1016/S0141-3910(99)00104-4.

[53] N.S. Allen, M. Edge, M. Mohammadian, K. Jones, Physicochemical aspects of the environmental degradation of poly(ethylene terephthalate), Polym Degrad Stab. 43 (1994) 229–237. https://doi.org/10.1016/0141-3910(94)90074-4.

[54] E. Pirzadeh, A. Zadhoush, M. Haghighat, Hydrolytic and thermal degradation of PET fibers and PET granule: The effects of crystallization, temperature, and humidity, J Appl Polym Sci. 106 (2007) 1544–1549. https://doi.org/10.1002/APP.26788.

[55] Y. Geng, T. Dong, P. Fang, Q. Zhou, X. Lu, S. Zhang, Fast and effective glycolysis of poly(ethylene terephthalate) catalyzed by polyoxometalate, Polym Degrad Stab. 117 (2015) 30–36. https://doi.org/10.1016/j.polymdegradstab.2015.03.019.

[56] Y. Kim, M. Kim, J. Hwang, E. Im, G.D. Moon, Optimizing PET Glycolysis with an Oyster Shell-Derived Catalyst Using Response Surface Methodology, Polymers (Basel). 14 (2022). https://doi.org/10.3390/polym14040656.

[57] R. López-Fonseca, I. Duque-Ingunza, B. de Rivas, L. Flores-Giraldo, J.I. Gutiérrez-Ortiz, Kinetics of catalytic glycolysis of PET wastes with sodium carbonate, Chemical Engineering Journal. 168 (2011) 312–320. https://doi.org/10.1016/j.cej.2011.01.031.

[58] Z. Laldinpuii, S. Lalhmangaihzuala, Z. Pachuau, K. Vanlaldinpuia, Depolymerization of poly(ethylene terephthalate) waste with biomass-waste derived recyclable heterogeneous catalyst, Waste Management. 126 (2021) 1–10. https://doi.org/10.1016/j.wasman.2021.02.056.

[59] M. Ghaemy, K. Mossaddegh, Depolymerisation of poly(ethylene terephthalate) fibre wastes using ethylene glycol, Polym Degrad Stab. 90 (2005) 570–576. https://doi.org/10.1016/j.polymdegradstab.2005.03.011.

[60] G. Xi, M. Lu, C. Sun, Study on depolymerization of waste polyethylene terephthalate into monomer of bis(2-hydroxyethyl terephthalate), Polym Degrad Stab. 87 (2005) 117–120. https://doi.org/10.1016/J.POLYMDEGRADSTAB.2004.07.017.

[61] S.R. Shukla, A.M. Harad, Glycolysis of polyethylene terephthalate waste fibers, J Appl Polym Sci. 97 (2005) 513–517. https://doi.org/10.1002/app.21769.

[62] C.H. Chen, Study of glycolysis of poly(ethylene terephthalate) recycled from postconsumer soft-drink bottles. III. Further investigation, J Appl Polym Sci. 87 (2003) 2004–2010. https://doi.org/10.1002/app.11694.

[63] A.S. Goje, S. Mishra, Chemical kinetics, simulation, and thermodynamics of glycolytic depolymerization of poly(ethylene terephthalate) waste with catalyst optimization for recycling of value added monomeric products, Macromol Mater Eng. 288 (2003) 326–336. https://doi.org/10.1002/mame.200390034.

[64] S. Lyu, D. Untereker, Degradability of polymers for implantable biomedical devices, Int J Mol Sci. 10 (2009) 4033–4065. https://doi.org/10.3390/ijms10094033.

[65] S. Lyu, J. Schley, B. Loy, D. Lind, C. Hobot, R. Sparer, D. Untereker, Kinetics and Time−Temperature Equivalence of Polymer Degradation Kinetics and Time-

Temperature Equivalence of Polymer Degradation, (2007). https://doi.org/10.1021/bm070313n.

[66] J.D. Badia, A. Martinez-Felipe, L. Santonja-Blasco, A. Ribes-Greus, Thermal and thermo-oxidative stability of reprocessed poly(ethylene terephthalate), J Anal Appl Pyrolysis. 99 (2013) 191–202. https://doi.org/10.1016/j.jaap.2012.09.003.

[67] G. Montaudo, C. Puglisi, F. Samperi, Primary thermal degradation mechanisms of PET and PBT, Polym Degrad Stab. 42 (1993) 13–28. https://doi.org/10.1016/0141-3910(93)90021-A.

[68] S. V. Levchik, E.D. Weil, A review on thermal decomposition and combustion of thermoplastic polyesters, Polym Adv Technol. 15 (2004) 691–700. https://doi.org/10.1002/PAT.526.

[69] D.-T. Van-Pham, Q.-H. Le, T.-N. Lam, C.-N. Nguyen, W. Sakai, Four-factor optimization for PET glycolysis with consideration of the effect of sodium bicarbonate catalyst using response surface methodology, Polym Degrad Stab. 179 (2020) 109257. https://doi.org/10.1016/j.polymdegradstab.2020.109257.

[70] I. Cano, C. Martin, J.A. Fernandes, R.W. Lodge, J. Dupont, F.A. Casado-Carmona, R. Lucena, S. Cardenas, V. Sans, I. de Pedro, Paramagnetic ionic liquid-coated SiO2@Fe3O4 nanoparticles—The next generation of magnetically recoverable nanocatalysts applied in the glycolysis of PET, Appl Catal B. 260 (2020) 118110. https://doi.org/10.1016/J.APCATB.2019.118110.

[71] Y. Hu, Y. Wang, X. Zhang, J. Qian, X. Xing, X. Wang, Synthesis of poly(ethylene terephthalate) based on glycolysis of waste PET fiber, Journal of Macromolecular Science, Part A. 57 (2020) 430–438. https://doi.org/10.1080/10601325.2019.1709498.

[72] F. Villain, J. Coudane, M. Vert, Thermal degradation of poly(ethylene terephthalate) and the estimation of volatile degradation products, Polym Degrad Stab. 43 (1994) 431–440. https://doi.org/10.1016/0141-3910(94)90016-7.

[73] K.S. Seo, J.D. Cloyd, Kinetics of hydrolysis and thermal degradation of polyester melts, J Appl Polym Sci. 42 (1991) 845–850. https://doi.org/10.1002/APP.1991.070420330.

[74] B.J. Holland, J.N. Hay, The thermal degradation of PET and analogous polyesters measured by thermal analysis–Fourier transform infrared spectroscopy, Polymer (Guildf). 43 (2002) 1835–1847. https://doi.org/10.1016/S0032-3861(01)00775-3.

[75] S. Mandal, A. Dey, PET Chemistry, Recycling of Polyethylene Terephthalate Bottles. (2019) 1–22. https://doi.org/10.1016/B978-0-12-811361-5.00001-8.

[76] F. Awaja, D. Pavel, Recycling of PET, Eur Polym J. 41 (2005) 1453–1477. https://doi.org/10.1016/J.EURPOLYMJ.2005.02.005.

[77] B. Demirel, A. Yaraş, H. Elçiçek, Crystallization Behavior of PET Materials, BAÜ Fen Bil. Enst. Dergisi Cilt. 13 (2011) 26–35. http://hdl.handle.net/11772/1592 (accessed July 22, 2022).

[78] J.D. Badia, F. Vilaplana, S. Karlsson, A. Ribes-Greus, Thermal analysis as a quality tool for assessing the influence of thermo-mechanical degradation on recycled poly(ethylene terephthalate), Polym Test. 28 (2009) 169–175. https://doi.org/10.1016/j.polymertesting.2008.11.010.

[79] R. Panowicz, M. Konarzewski, T. Durejko, M. Szala, M. Łazińska, M. Czerwińska, P. Prasuła, Properties of Polyethylene Terephthalate (PET) after Thermo-Oxidative Aging, Materials 2021, Vol. 14, Page 3833. 14 (2021) 3833. https://doi.org/10.3390/MA14143833.

[80] T. Yamada, Y. Mizuno, Y. Imamura, Measurement of the melting points of oligomers obtained in the manufacture of poly(ethylene terephthalate), Polym Eng Sci. 28 (1988) 377–380. https://doi.org/10.1002/PEN.760280606.

[81] A. Launay, F. Thominette, J. Verdu, Hydrolysis of poly(ethylene terephthalate): a kinetic study, Polym Degrad Stab. 46 (1994) 319–324. https://doi.org/10.1016/0141-3910(94)90148-1.

[82] G.E. Sweet, J.P. Bell, Multiple endotherm melting behavior in relation to polymer morphology, Journal of Polymer Science Part A-2: Polymer Physics. 10 (1972) 1273–1283. https://doi.org/10.1002/POL.1972.160100707.

[83] R.C. Roberts, Poly(ethylene terephthalate) II—Morphological changes on annealing, Polymer (Guildf). 10 (1969) 117–125. https://doi.org/10.1016/0032-3861(69)90015-9.

[84] S. Tan, A. Su, W. Li, E. Zhou, New Insight into Melting and Crystallization Behavior in Semicrystalline Poly(ethylene terephthalate), J Polym Sci B: Polym Phys. 38 (2000) 53–60. https://doi.org/10.1002/(SICI)1099-0488(20000101)38:1.

[85] J.D. Badia, E. Strömberg, S. Karlsson, A. Ribes-Greus, The role of crystalline, mobile amorphous and rigid amorphous fractions in the performance of recycled poly (ethylene terephthalate) (PET), Polym Degrad Stab. 97 (2012) 98–107. https://doi.org/10.1016/j.polymdegradstab.2011.10.008.

[86] L. Santonja-Blasco, R. Moriana, J.D. Badía, A. Ribes-Greus, Thermal analysis applied to the characterization of degradation in soil of polylactide: I. Calorimetric and viscoelastic analyses, Polym Degrad Stab. 95 (2010) 2185–2191. https://doi.org/10.1016/j.polymdegradstab.2010.08.005.

[87] S. Baliga, W.T. Wong, Depolymerization of poly(ethylene terephthalate) recycled from post-consumer soft-drink bottles, J Polym Sci A Polym Chem. 27 (1989) 2071–2082. https://doi.org/10.1002/POLA.1989.080270625.

[88] M. Imran, B.K. Kim, M. Han, B.G. Cho, D.H. Kim, Sub- and supercritical glycolysis of polyethylene terephthalate (PET) into the monomer bis(2-hydroxyethyl) terephthalate (BHET), Polym Degrad Stab. 95 (2010) 1686–1693. https://doi.org/10.1016/J.POLYMDEGRADSTAB.2010.05.026.

[89] J.C. Viana, L. Todorov, Structure-Properties Relationships in Processed Poly(ethylene terephthalate), Key Eng Mater. 554–557 (2013) 1757–1762. https://doi.org/10.4028/WWW.SCIENTIFIC.NET/KEM.554-557.1757.

[90] Y. Fu, B. Annis, A. Boller, Y. Jin, B. Wunderlich, Analysis of structure and properties of poly(ethylene terephthalate) fibers, J Polym Sci B Polym Phys. 32 (1994) 2289–2306. https://doi.org/10.1002/POLB.1994.090321316.

[91] V.B. Gupta, Some developments in poly(ethylene terephthalate) fibre production and structure-property relationships, Indian J Fibre Text Res. 20 (1995) 43–59. http://nopr.niscpr.res.in/handle/123456789/32299 (accessed September 16, 2022).

[92] R. Rastogi, W.P. Vellinca, S. Rastogi, C. Schick, H.E.H. Meijer, The three-phase structure and mechanical properties of poly(ethylene terephthalate), J Polym Sci B Polym Phys. 42 (2004) 2092–2106. https://doi.org/10.1002/POLB.20096.

C. Primaz, O. Gil-Castell, A. Ribes-Greus. Partial glycolytic depolymerisation of poly(ethylene terephthalate) (PET) in the solid state: modelling the contribution of time and temperature. Polymer Degradation and Stability 2024:221;110695